

Stress Change Calculations in Accidentally Damaged Prestressed Bridge Girders

Habib Tabatabai

University of Wisconsin – Milwaukee
3200 N Cramer St
Milwaukee, WI, 53211 USA
Email: ht@uwm.edu (corresponding author)
Tel No.: 1-414-229-5166

Azam Nabizadeh

University of Wisconsin – Milwaukee
3200 N Cramer St
Milwaukee, WI, 53211 USA
Email: azam@uwm.edu

Abstract: Accidental damage to prestressed concrete bridge girders may occur due to impact by over-height vehicles on the bottom of the girder, or the top flange of the girder may be damaged during deck removal and replacement operations. Since stress checks at service loads are an important component of design for prestressed concrete beams, serviceability-based stress checks should be considered when assessing the structural condition of damaged girders. In this paper, step-by-step theoretical calculations are used to develop equations for estimating service load stress changes due to physical damage (partial loss of concrete section and strands) based on a differential approach. The effects of lack of symmetry in the damaged cross section is considered in the calculations. A spreadsheet-based program is developed to calculate complex section property values for the damaged sections. The accuracy of the developed equations was verified using a finite element model of a prestressed beam under undamaged and damaged conditions. Reasonably good agreement was noted between the predicted stress changes and the finite element results.

Keywords: Bridges, prestressed concrete, damage, over-height truck, serviceability, stresses.

Citation: Tabatabai, H., Nabizadeh, A., “Stress Change Calculations in Accidentally Damaged Prestressed Bridge Girders,” Bridge Structures, IOS Press, 2022, DOI:10.3233/BRS-220197

1.0 BACKGROUND

Accidental damage causes serious damage to prestressed concrete bridges in the United States [1]. There are three primary modes of accidental damage to prestressed concrete bridge girders:

1. Accidental impact damage due to over-height vehicles, primarily at the bottom flange and web areas (Figure 1a).
2. Unintended construction-related damage during deck removal processes, primarily at the top flange area. (Figure 1b).

When faced with an accidental damage, an engineer may need to first make emergency decisions regarding public safety, stabilization of the situation, and possible restriction of access to the bridge (top or underside) based on the initial (limited) observations of the damage. The next step would be to obtain relevant information about the damaged girder(s) including material properties, geometry, and reinforcement. The extent and severity of damage must then be assessed. This assessment is generally made using visual inspections. However, hand calculations or computer analyses may also be performed to further clarify the nature and extent of damage, and to help develop proper repair procedures. Such analyses must consider both serviceability and strength limit states. The repairs should restore acceptable serviceability and strength condition and result in durable service during the remaining service life of the bridge.

Impact damage can range from minor scrapes to severe structural damage, mostly occurring in the exterior girder. However, damage to interior girders could also occur as the vehicle may bounce back after initial impact. Impact damage can affect both the concrete and pre-stressing strands. Impact damage caused by over-height vehicles is usually located in the middle one-third region of the girders.

This paper addresses service stress calculations in damaged prestressed girders and proposes computational methods and calculation procedures to assess the effects of damage. This work is derived from a larger research report by Tabatabai and Nabizadeh [2].

Detailed information is available in the literature regarding accidental damage to prestressed girders due to over-height vehicles. Various researchers have proposed guidelines that address damage assessments and classification as well as specific repair techniques and procedures for a variety of damage conditions. The most recent example is a comprehensive study of this subject for the Wisconsin Department of Transportation [2,3]. Previous major works include NCHRP Report 280 [1], NCHRP Report 226 [4], Tadros and Baishya [5], Harries [6], Harries et al. [7], Assad [8], and a PhD dissertation by Kassan [9]. However, these studies (other than the report by Tabatabai and Nabizadeh [2]) do not address the problem of estimating service stresses in damaged prestressed girders, and do not provide detailed procedures or software regarding the various aspects of assessment and repair of damage.

Tabatabai and Nabizadeh [2] developed comprehensive procedures for assessment and repair of damaged prestressed bridge girders due to accidental damage to top or bottom flanges of prestressed concrete bridge girders for the Wisconsin Department of Transportation. The report recommends calculation procedures and recommended repairs (including splicing and FRP repairs) based on a new set of classification criteria for various types and extent of damage. The NCHRP Report 226 provides general guidelines for assessment, inspection, and repair. The report classifies damage as minor, moderate, and severe. In NCHRP Report 280, some of the repair methods discussed in the NCHRP Report 226 were load-tested and detailed recommendations for their applications were given. Guidelines were proposed based on serviceability conditions, strength, fatigue life, durability, cost, user inconvenience, speed of repairs, aesthetics, and range of applicability [9].

Feldman et al. [10] assessed impact damage reports for the Texas DOT while Harries et al. [7] investigated repair methods for prestressed bridges in a major report to the Pennsylvania DOT. Harries et al. [7] discussed the NCHRP 280 report and reviewed their assessment processes. The authors also conducted a survey of practice in North America. The authors investigated different repair methods including CFRP repairs, strand splicing and steel post tensioning repairs.

Assad [8] investigated different deck removal methods and their effect on the performance of the prestressed girder with wide and narrow top flanges. The author studied saw cutting and jackhammering techniques as well as cost, duration, and environmental impact of each method. The author studied the effect of reducing 50% of the width of top flange for cases with different span-to-depth ratios.

2.0 METHODOLOGY

2.1 Stress Calculations in Damaged Prestressed Girders

The design of prestressed concrete girders for buildings and bridges consists of two primary design considerations, both of which are based on sectional analyses at critical sections: 1) stress checks at the serviceability limit state, and 2) strength check at the strength limit state. Typically, the number and layout of prestressing steel strands are selected to meet the tension and compression stress limits under the applicable serviceability-based load combination(s), and then strength checks are made for the strength-based load combinations.

The calculation of stresses (on any desired section) and checking those stresses against the corresponding allowable limits specified by the building and bridge design codes are well-established and straightforward for undamaged prestressed girders. In undamaged cases, there is at least one axis of symmetry present, thus the basic bending stress equation is applicable. The stresses at critical locations due to prestressing and girder self-weight are calculated at the “initial” state (in prestressing plant right after de-tensioning), and later when the girder is placed on the structure (following prestress losses). The non-composite girder section properties are used to calculate stresses based on the general linear stress relationship shown below:

$$\sigma = \frac{P}{A} \pm \frac{Pey}{I} \pm \frac{My}{I}$$

Where σ is the bending stress at any point y (vertical distance from the horizontal axis through the centroid), A is the cross-sectional area, e is the eccentricity of prestressing force from the centroid (along the y axis), M is the applied moment, and I is the moment of inertia with respect to the principal horizontal axis. Following the installation of girder on site, the stress imposed by the weight of the fresh concrete slab is

also applied on the non-composite girder properties, while the subsequent composite dead loads and live loads are applied on the composite section (with a composite moment of inertia), using the same basic flexural stress equation.

In a composite prestressed concrete girder/slab system (where girder is not shored during construction), the dead loads due to the weight of the girder and the concrete slab are resisted by the non-composite section, and the slab would theoretically not sustain any dead load stresses except for dead loads that are subsequently applied on the composite section. However, in a composite prestressed girder under dead load, any damage to the girder would redistribute the existing dead load stresses, and these stresses would shift into the slab as well. To estimate the change in stresses due to loss of section, a set of analytical procedures must be developed.

The process to calculate service level stresses when a part of the cross section is lost is not well established. Most researchers studying damaged prestressed bridge girders have focused on calculating and restoring sectional (and member) strength (such as Harries et al. [11]), and not assessing whether service stresses would in fact remain within the allowable limits. This is due mainly to the complexity of assessing the effects of loss of section on the state of stress within the post-loss section. Shanafelt and Horn [1] tried to bracket the problem of estimating stresses following damage by assuming that the girder and slab dead load could be resisted by the girder alone, or by the full composite section, and thus finding the range of possible stress values.

The problem of finding changes in stresses due to section loss in a composite (or non-composite) section while under existing dead load stresses is a complicated problem. In this paper, a methodology is proposed to estimate such changes in stress because of damage.

The sequence of dead load stress calculations when the girder is damaged in the bottom flange zone is as follows:

- 1) Calculate stresses (at various points in the cross section) due to prestress and girder dead load at the time of deck placement
- 2) Add (to Step 1) stresses due to deck slab weight ($\sigma=Mc/I$, using non-composite I)
- 3) Add (to Step 2) stresses due to composite dead loads (using composite moment of inertia)
- 4) Calculate changes in stress due to loss of section (concrete and/or prestressing steel). The stresses following damage would be equal to the stresses in Step 3 plus changes calculated in Step 4.
- 5) Calculate stress changes following repair: preloading (if applicable), patching, and CFRP repair (if any). If preloading is not applied, there would not be any change in dead load stresses following repairs.

The sequence of dead load stress calculations for top damage cases is as follows:

- 1) Calculate stresses (at various point in the cross section) due to prestress and girder dead load at the time of deck placement
- 2) Add (to Step 1) stresses due to deck slab weight ($\sigma=Mc/I$, using non-composite I)
- 3) Add (to Step 2) stresses due to composite dead loads (using composite moment of inertia)
- 4) Remove slab and other dead loads except the girder dead load. Stress due to girder dead weight on the non-composite girder section would remain.
- 5) Calculate changes in stress due to loss of section (in the top flange of the girder) and add to stresses in Step 4 to arrive at post-damage stresses.
- 6) Calculate stress changes following repair: preloading (if applicable), patching, etc.

In the following sections, a set of incremental procedures are developed for calculating the changes in stress due to damage. First, the concept of transformed section is discussed to implicitly account for prestress losses and gains when calculating stresses. Then the effect of section loss is considered with or without a deck slab (an additional area that is initially unstressed under dead load). Later, a differential form of the general bending equation is used to estimate changes in stress. To verify the analysis procedure, the results are then compared with finite element results for a specific example.

2.2 Concentrically prestressed sections

To set the stage for the proposed methodology, it is informative to consider a few simple examples involving sections with a concentric prestressing force applied at the geometric center of the section. Figure 2 shows a rectangular concrete cross section ($b \times h$) with a prestressing tendon (with area A_s) located at the centroid of the section. In the following calculations, stresses due to the application of the prestressing force are calculated using non-transformed and transformed sections.

2.2.1 Analysis using transformed and non-transformed sections

Assume that P_i is the initial prestress force applied on a cross section using a prestressing tendon with an area A_s on a concrete area A_c . The prestressing steel and concrete are bonded together (i.e., compatibility of strains between the two apply).

$$A_c = bh - A_s$$

If non-transformed area is used (i.e., the prestressing steel area is not converted into an equivalent concrete area using the modular ratio $n = \frac{E_s}{E_c}$), the initial stress in concrete (σ_1) is:

$$\sigma_1 = \frac{P_i}{A_c}$$

$$\text{Define: } x = \frac{E_s A_s}{E_c A_c} = n\rho$$

where ρ is the reinforcement ratio (A_s/A_c), and E_s and E_c are the moduli of elasticity for prestressing steel and concrete, respectively.

Because of the application of σ_1 , and the resulting compressive strain in concrete, the corresponding strain in the steel is reduced due to compatibility, and the prestressing force is also reduced. This causes a change in the stress in concrete due to elastic shortening, with the stresses in steel and concrete changing subsequently in an iterative process:

$$\sigma_2 = \sigma_1 - \frac{\sigma_1 E_s}{E_c A_c} A_s = \sigma_1 - \sigma_1 x$$

Similarly, the reduction in concrete stress causes an increase in the steel stress:

$$\sigma_3 = \sigma_2 - \frac{\sigma_2 - \sigma_1}{E_c} \frac{E_s}{A_c} A_s = \sigma_2 + \sigma_1 x^2 = \sigma_1 - \sigma_1 x + \sigma_1 x^2$$

...

$$\sigma_m = \sigma_1 - \sigma_1 x + \sigma_1 x^2 - \sigma_1 x^3 + \sigma_1 x^4 + \dots + \sigma_1 x^{m-1} - \sigma_1 x^m$$

This process can be rewritten in the following form:

$$\sigma_m = \sigma_1 (1 - x + x^2 - x^3 + x^4 + \dots + x^{m-1} - x^m) = \sigma_1 S_m$$

where

$$S_m = 1 - x + x^2 - x^3 + x^4 + \dots + x^{m-1} - x^m$$

$$xS_m = x - x^2 + x^3 - x^4 + x^5 + \dots + x^m - x^{m+1}$$

Adding the above two expressions result in:

$$S_m + xS_m = S_m(1 + x) = 1 - x^{m+1}$$

Considering that the value of the modular ratio n is generally on the order of 8 to 9, and A_c is far larger than A_s , x is typically a number that is less than 1.

$$\text{Therefore, since } x < 1 \Rightarrow \lim_{m \rightarrow \infty} (1 - x^{m+1}) = 1.0 \Rightarrow S_m = \frac{1}{1+x}$$

$$\Rightarrow \sigma_{final} = \sigma_f = \sigma_1 \left(\frac{1}{1+x} \right) = \sigma_1 \left(\frac{1}{1+n\rho} \right) = \frac{A_c}{A_c + nA_s} \sigma_1 \quad (1)$$

Now consider a transformed cross section in which the prestressing steel is converted into an equivalent concrete (Figure 3). Therefore, the transformed cross-sectional area is $(A_c + nA_s)$. The final stress can be determined without iteration:

$$\sigma_f = \frac{P_i}{A_c + nA_s} = \frac{P_i}{A_c} \frac{A_c}{A_c + nA_s} = \sigma_1 \frac{A_c}{A_c + nA_s} \quad (2)$$

Equations 1 and 2 are identical. This illustrates that, to avoid iteration and to avoid explicitly accounting for elastic shortening loss (or gain) when calculating stresses, a transformed section can be used [12]. A similar approach can be taken to address stress change due to loss of section as indicated below.

2.2.2 Symmetrical Loss of section

The following simple example illustrates the effect of loss of cross section. Assume that the cross-sectional area of the concrete section in the previous example suffers a symmetrical loss of cross-sectional area (A_d) (cross hatched) as shown in Figure 4.

$$A_d = \text{loss of section due to damage}$$

The transformed areas are used here to avoid calculating elastic losses and gains. The transformed cross-sectional area in undamaged (A_t) and damaged sections (A'_t) can be calculated as follows:

$$A_t = bh - A_s + nA_s = A_c + nA_s$$

$$A'_t = bh - A_s - A_d + nA_s = A'_c + nA_s$$

$$\text{where } A'_c = A_c - A_d$$

The stress that exists before occurrence of damage is:

$$\sigma_1 = \frac{P_u}{A_t}$$

where, P_u is the prestressing force before damage occurs (undamaged).

Due to loss of section, a change in stress occurs:

$$\sigma'_1 = \frac{P_u}{A'_t} - \frac{P_u}{A_t} = P_u \left(\frac{1}{A'_t} - \frac{1}{A_t} \right) = \frac{A_t - A'_t}{A'_t A_t} P_u$$

$$\sigma'_1 = P_u \frac{(A_c + nA_s) - (A'_c + nA_s)}{(A_c + nA_s)(A'_c + nA_s)} = \frac{A_c - A'_c}{(A_c + nA_s)(A'_c + nA_s)} P_u = \frac{A_d}{A'_t A_t} P_u \quad (3)$$

This change in stress due to loss of section causes prestress losses (elastic gain or loss) that are directly accounted for when using transformed sections (as discussed in the example above).

The change in stress can also be calculated using a differential approach. Using transformed sections to avoid elastic gain/loss calculations, the basic stress relationship can be written as:

$$\sigma = \frac{P_u}{A_t} \quad (4)$$

$$\Delta\sigma = \frac{(\Delta P_u)(A_t) - (\Delta A_t)P_u}{A_t^2}$$

Since transformed section properties are used, ΔP_u can be set equal to zero. Thus,

$$\Delta\sigma = \frac{-(\Delta A_t)P_u}{A_t^2}$$

The total stress = $\sigma_1 + \Delta\sigma$

However, the change in A_t or (ΔA_t) is equal to the loss in sectional area or A_d . Substituting A_d for ΔA_t ,

$$\Delta\sigma = -\frac{A_d P_u}{(A_t)^2} \quad (5)$$

Equation 3 approaches Equation 5 when A_d is small. The differential form may be used to calculate stress change when A_d is relatively small. However, as damage gets larger, Equation 5 would be expected to lose accuracy (the differential solution may not apply). Equation 3 may be used in such cases.

2.2.3 Section gain

In the previous example, the effect of loss of cross-sectional area on stresses was discussed. The same discussion can be made regarding a sectional gain (increase in cross-sectional area). In this example, assuming that the prestress force was applied on the original (non-augmented) section, the subsequent addition of an area (area gain or A_g) to the section would not redirect stresses to the new areas. This is analogous to adding a deck area on the girder, which would remain stress free without the action of creep, shrinkage, and composite dead loads. In a composite prestressed girder/slab system, the addition of slab augments the beam area without a redistribution of the stresses that already exist in the girder alone. If a subsequent loss of section (A_d) occurs, it would not be immediately clear how existing forces would be redistributed in the composite section ($A_c + nA_s + A_g$). It is assumed here that both the gain and loss areas occur symmetrically with respect to the original section (Figure 5).

For this condition, Equation 3 can be rewritten in the following form to calculate stress change due to damage A_d

$$\Delta\sigma = -\frac{A_d P_u}{(A_c + nA_s)(A_c + A_g - A_d + nA_s)} = \frac{A_d P_u}{(A_t)(A'_{tc})} \quad (6)$$

where A'_{tc} is the transformed composite (damaged) area. The differential approach proposed can be extended to unsymmetrical sections (including eccentric prestressing force) and moments.

2.3 Eccentrically prestressed section

In the previous section, examples involving a concentric prestressing force applied on a section was presented. In this section, it is illustrated that the use of the transformed section can similarly eliminate the need for iteration for prestress losses (and gains) when the prestress force is eccentric with respect to the centroid of the cross section (Figure 6).

In addition to the parameters defined earlier,

I_c = moment of inertia of concrete section

c = distance from the top fiber to the centroid of the concrete section.

e_c = eccentricity of prestressing force relative to the centroid of concrete section.

Using the non-transformed section, the initial flexural stress at the centroid of prestressing force can be calculated as

$$\sigma_1 = \frac{P_i}{A_c} + \frac{P_i e_c^2}{I_c}$$

This level of stress causes a strain in concrete $\frac{\sigma_1}{E_c}$, which in turn causes a loss in prestressing steel due to strain compatibility ($\frac{\sigma_1}{E_c} E_s$). The stress in concrete at the centroid of steel would then become:

$$\sigma_2 = \sigma_1 - \frac{\sigma_1}{E_c} E_s A_s \left(\frac{1}{A_c} + \frac{e_c^2}{I_c} \right)$$

$$\text{Define } x = \frac{E_s A_s}{E_c} \left(\frac{1}{A_c} + \frac{e_c^2}{I_c} \right)$$

$$\sigma_2 = \sigma_1 - \sigma_1 x$$

This would further change both the steel and concrete stresses in an iterative fashion.

$$\sigma_3 = \sigma_1 - \sigma_1 x + \sigma_1 x^2$$

...

$$\sigma_m = \sigma_1 - \sigma_1 x + \sigma_1 x^2 - \sigma_1 x^3 + \dots + \sigma_1 x^{m-1} - \sigma_1 x^m = \sigma_1 (1 - x + x^2 - x^3 + \dots + x^{m-1} - x^m)$$

As discussed earlier, the limit for the above series ($1 - x + x^2 - x^3 + \dots + x^{m-1}$) is equal to $\frac{1}{1+x}$, therefore, the final stress is:

$$\sigma_{final} = \sigma_1 \left(\frac{1}{1+x} \right) = \left[\frac{P_i}{A_c} + \frac{P_i e_c^2}{I_c} \right] \left[\frac{1}{1 + n A_s \left(\frac{1}{A_c} + \frac{e_c^2}{I_c} \right)} \right]$$

$$\sigma_{final} = \left[\frac{P_i}{A_c} + \frac{P_i e_c^2}{I_c} \right] \left[\frac{1}{\frac{A_c I_c + n A_s I_c + n A_s e_c^2 A_c}{A_c I_c}} \right]$$

$$\begin{aligned}
\sigma_{final} &= \left[\frac{P_i}{A_c} + \frac{P_i e_c^2}{I_c} \right] \left[\frac{A_c I_c}{I_c (A_c + nA_s) + nA_s e_c^2 A_c} \right] \\
&= \left[\frac{P_i}{A_c} + \frac{P_i e_c^2}{I_c} \right] \left[\frac{1}{\frac{I_c + nA_s e_c^2}{I_c} + \frac{nA_s}{A_c}} \right] \\
\sigma_{final} &= P_i \left(\frac{I_c + A_c e_c^2}{A_c I_c} \right) \left(\frac{A_c I_c}{A_c (I_c + nA_s e_c^2) + nA_s I_c} \right) \\
\sigma_{final} &= P_i \left(\frac{I_c + A_c e_c^2}{A_c (I_c + nA_s e_c^2) + nA_s I_c} \right) \\
\sigma_{final} &= P_i \left(\frac{I_c + A_c e_c^2}{(I_c (A_c + nA_s) + nA_s A_c e_c^2)} \right) \tag{7}
\end{aligned}$$

Now, using the transformed section properties, the following can be written:

$$A_c = bh - A_s$$

$$c_t = \frac{cA_c + nA_s d}{A_c + nA_s}$$

where c_t is the distance from the top fiber to the neutral axis of the transformed section, and $e_{tc} = d - c_t$

$$\text{Therefore, } e_{tc} = d - \frac{cA_c + nA_s d}{A_c + nA_s} = \frac{dA_c + nA_s d - cA_c - nA_s d}{A_c + nA_s}$$

$$e_{tc} = \frac{A_c (d - c)}{A_c + nA_s}$$

$$\text{Since } e_c = d - c \Rightarrow e_{tc} = \frac{A_c e_c}{A_c + nA_s}$$

Using parallel axis theorem, the transformed moment of inertia of section can be calculated as follows:

$$I_{tc} = I_c + A_c (e_c - e_{tc})^2 + nA_s (e_{tc})^2$$

$$I_{tc} = I_c + A_c \left(e_c - \frac{A_c e_c}{A_c + nA_s} \right)^2 + nA_s \left(\frac{A_c e_c}{A_c + nA_s} \right)^2$$

$$I_{tc} = I_c + A_c \left(\frac{A_c e_c + nA_s e_c - A_c e_c}{A_c + nA_s} \right)^2 + nA_s \left(\frac{A_c e_c}{A_c + nA_s} \right)^2$$

$$I_{tc} = I_c + \frac{A_c (n^2 A_s^2 e_c^2)}{(A_c + nA_s)^2} + \frac{nA_s (A_c^2 e_c^2)}{(A_c + nA_s)^2}$$

$$I_{tc} = I_c + \frac{e_c^2 A_c}{A_c + nA_s} \frac{n^2 A_s^2 + nA_s A_c}{A_c + nA_s}$$

$$= I_c + \frac{e_c^2 A_c}{A_c + nA_s} \frac{nA_s (A_c + nA_s)}{A_c + nA_s}$$

$$\begin{aligned}
&= I_c + \frac{nA_s e_c^2 A_c}{(A_c + nA_s)} = I_c + nA_s \frac{A_c}{(A_c + nA_s)} e_c^2 \\
A_{tc} &= A_c + nA_s \\
\sigma_{final} &= \frac{P_i}{A_{tc}} + \frac{P_i e_{tc}^2}{I_{tc}} \\
&= \frac{P_i}{A_c + nA_s} + \frac{P_i \left(\frac{A_c}{A_c + nA_s} \right)^2 e_c^2}{I_c + nA_s \left(\frac{A_c}{A_c + nA_s} \right) e_c^2} \\
&= P_i \frac{I_c + nA_s \left(\frac{A_c}{A_c + nA_s} \right) e_c^2 + \left(\frac{A_c}{A_c + nA_s} \right)^2 e_c^2 (A_c + nA_s)}{(A_c + nA_s) \left(I_c + nA_s \left(\frac{A_c}{A_c + nA_s} \right) e_c^2 \right)} \\
&= P_i \frac{I_c + \left(\frac{nA_s A_c}{A_c + nA_s} \right) e_c^2 + A_c^2 e_c^2 \left(\frac{1}{A_c + nA_s} \right)}{I_c (A_c + nA_s) + nA_s A_c e_c^2} \\
&= P_i \frac{I_c + \left(\frac{nA_s A_c e_c^2 + A_c^2 e_c^2}{A_c + nA_s} \right)}{I_c (A_c + nA_s) + nA_s A_c e_c^2} \\
&= P_i \frac{I_c + A_c e_c^2}{I_c (A_c + nA_s) + nA_s A_c e_c^2} \tag{8}
\end{aligned}$$

Equation 7 and Equation 8 are identical indicating that the use of transformed section can eliminate the need for iterations to calculate stresses due to prestress gains and losses. Similar approach can be extended to section losses, section gains, and losses after section gain as discussed earlier under the case of concentric prestress force.

2.4 Differential approach for calculating changes in bending stress due to section loss

In a cross section with at least one axis of symmetry, a generic linearly elastic equation for bending stress (σ) can be written as a function of applied moment (M), distance to desired location for bending stress calculation (y), and moment of inertia (I):

$$\sigma = \frac{My}{I} \tag{9}$$

The change in stress due to damage can be written in a differential form:

$$\Delta\sigma = \frac{((\Delta M)y + M(\Delta y))I - (\Delta I)(My)}{I^2} \quad (10)$$

Although the externally applied moment may remain essentially unchanged, and elastic loss/gain are implicitly accounted for, the change in the position of neutral axis can modify the moment due to prestressing. In the above equation, Δy is the change in position of the desired point with respect to the neutral axis, (which shifts because of damage) and, ΔI is the change in the moment of inertia because of damage.

To account for the elastic gain or loss effects implicitly, the transformed section properties should be used (steel converted to equivalent concrete). Furthermore, the state of the cross section at the time of damage should be the basis for the type of section properties used. For example, If the cross section is a composite of a prestressed girder and a slab, the I , ΔI , y and Δy parameters should be based on the composite transformed section properties.

In Equation 10, it is assumed that any damage would occur such that at least one axis of symmetry would remain in the beam cross section. When the section has no axis of symmetry, or when the damage causes the section to become non-symmetrical, the basic bending equation presented above would not be valid. The basic equation for calculating bending stress under biaxial bending in an unsymmetrical section at a point (x, y) is:

$$\sigma = \frac{M_y I_x - M_x I_{xy}}{I_x I_y - I_{xy}^2} x + \frac{M_x I_y - M_y I_{xy}}{I_x I_y - I_{xy}^2} y \quad (11)$$

where M_x and M_y are applied bending moments about the horizontal (x) and vertical (y) axes through the centroid of the cross-section, I_x and I_y are moments of inertia in the horizontal and vertical direction, and I_{xy} is the product of inertia. This equation would become the same as *Equation 9* when $M_y = 0$ and $I_{xy} = 0$.

The differential form of *Equation 11* can be written as follows:

$$\Delta\sigma = \left(\frac{\widehat{D} - \widehat{E}\widehat{A}}{\widehat{B}^2} \right) x + \left(\frac{\widehat{B}\widehat{F} - \widehat{E}\widehat{C}}{\widehat{B}^2} \right) y$$

where

$$\widehat{A} = M_y I_x - M_x I_{xy}$$

$$\widehat{B} = I_x I_y - I_{xy}^2$$

$$\widehat{C} = M_y I_y - M_x I_{xy}$$

$$\widehat{D} = x[\Delta M_y I_x + M_y \Delta I_x - \Delta M_{xx} I_{xy} - M_x \Delta I_{xy}] + \Delta x \widehat{A}$$

$$\widehat{E} = \Delta I_x (I_y) + I_x (\Delta I_y) - 2 I_{xy} (\Delta I_{xy})$$

$$\widehat{F} = y[\Delta M_x I_y + M_x \Delta I_y - \Delta M_y I_{xy} - M_y \Delta I_{xy}] + \Delta y \widehat{C}$$

In addition to the effects of biaxial external bending moment, the effect of prestressing must also be considered by adding the following stress components to the basic bending equation given in Equation 11.

The change in stress due to the prestressing force can then be

$$\sigma = \frac{P}{A} + \left(\frac{(P e_y) y}{I_x} \right) + \left(\frac{(P e_x) x}{I_y} \right)$$

$$\Delta\sigma = \frac{\Delta P A - \Delta A P}{A^2} + \frac{\left(\Delta P e_y y + P(\Delta e_y y + \Delta y e_y) \right) I_x - \Delta I_x P e_y y}{I_x^2} + \frac{\left(\Delta P e_x x + P(\Delta e_x x + \Delta x e_x) \right) I_y - \Delta I_y P e_x x}{I_y^2}$$

2.5 Generalized differential approach

The generalized equation for calculating stress under the biaxial effects of prestressing force and biaxial external bending moments on a section without any axis of symmetry (as in a damaged girder) can be calculated using the following equation:

$$\sigma = \frac{P}{A} + \left[\frac{(M_x + M_{Px}) I_y - (M_y + M_{Py}) I_{xy}}{I_x I_y - I_{xy}^2} \right] y + \left[\frac{(M_y + M_{Py}) I_x - (M_x + M_{Px}) I_{xy}}{I_x I_y - I_{xy}^2} \right] x \quad (12)$$

where M_x and M_y are the total external moments about the x and y axes, due to imposed dead and/or live loads, and M_{Px} and M_{Py} are moments due to eccentricity of axial force with respect to horizontal and vertical axes, respectively. The coordinates of the point for which the stress is being assessed is x and y.

Furthermore, $M_{Px} = P e_y$ and $M_{Py} = P e_x$

where e_x and e_y are the eccentricities of prestressing force (P) with respect to the y and x -axes, respectively, and I_{xy} is the product of inertia.

The change in stress due to changes in the cross-sectional properties (as in loss of section) can be estimated using the differential form (based on Equation 12):

$$\Delta\sigma = \Delta\sigma_1 + \Delta\sigma_2 + \Delta\sigma_3 \quad (13)$$

$$\Delta\sigma_1 = \frac{(\Delta P)A_t - (\Delta A)P}{(A_t)(A'_{tc})}$$

$$\Delta\sigma_2 = \left(\frac{\bar{B}\bar{F} - \bar{E}\bar{C}}{\bar{B}^2} \right) y + (\Delta y) \left(\frac{\bar{C}}{\bar{B}} \right)$$

$$\Delta\sigma_3 = \left(\frac{\bar{B}\bar{D} - \bar{E}\bar{A}}{\bar{B}^2} \right) x + (\Delta x) \left(\frac{\bar{A}}{\bar{B}} \right)$$

$$\bar{A} = (M_y + M_{Py})I_x - (M_x + M_{Px})I_{xy}$$

$$\bar{B} = I_x I_y - I_{xy}^2$$

$$\bar{C} = (M_x + M_{Px})I_y - (M_y + M_{Py})I_{xy}$$

$$\bar{D} = \left[\left((\Delta M_y) + (\Delta M_{Py}) \right) I_x + (M_y + M_{Py})(\Delta I_x) - \left((\Delta M_x) + (\Delta M_{Px}) \right) I_{xy} - (M_x + M_{Px})(\Delta I_{xy}) \right]$$

$$\bar{E} = (\Delta I_x)I_y + I_x(\Delta I_y) - 2I_{xy}(\Delta I_{xy})$$

$$\bar{F} = \left[(\Delta M_x + \Delta M_{Px})I_y + (M_x + M_{Px})(\Delta I_y) - (\Delta M_y + \Delta M_{Py})I_{xy} - (M_y + M_{Py})(\Delta I_{xy}) \right]$$

$$\Delta M_{Px} = (\Delta P)e_y + P(\Delta e_y)$$

$$\Delta M_{Py} = (\Delta P)e_x + P(\Delta e_x)$$

3.0 RESULTS

3.1 Suggested procedures for calculating change in stress due to damage

The suggested procedures for calculating changes in stress due to top and bottom damage cases are described below. Both cases utilize Equation 13 for calculating the change in stress. In both cases, all parameters related to section properties must be calculated for both undamaged and damaged states. When the structure undergoes change from an undamaged to damaged state, the non-differential parameters refer

to the undamaged state (just prior to damage) and the differential terms relate to the difference between damaged and undamaged states.

$$\Delta(\text{Parameter}) = (\text{Parameter})_{\text{Damaged}} - (\text{Parameter})_{\text{Undamaged}}$$

For bottom damage cases, the non-differential terms in Equation 13 refer to the properties of the undamaged properties of the composite girder/concrete slab, and the differential terms refer to the change between damaged and undamaged composite states. In top damage cases, the non-differential terms relate to the non-composite undamaged girder properties, and the differential terms address changes between damaged and undamaged non-composite conditions.

The determination of damaged section properties needed to calculate stresses using Equation 13 is complicated. To address this issue, a spreadsheet-based program was developed (PreBARS - Prestressed Bridge Assessment, Repair, and Strengthening). The geometry of the section was generated using spreadsheet cells as shown in Figure 7. Each cell represented a 0.5 in x 0.5 in square (12.7 mm x 12.7 mm) with different material properties associated with it (girder concrete, deck concrete, strand, patch material). Damage was introduced by simply erasing the cell contents in damaged areas. In concrete, areas that are spalled or cracked would be removed. The spreadsheet would then calculate undamaged and damaged section properties for use in Equation 13. Further details about PreBARS are presented by Tabatabai and Nabizadeh [2]. Using the PreBARS program, the authors performed several case studies on two example prestressed I-girder bridges, one with a long span (146 ft or 44.5 m) and the other with a short span (50 ft or 15.24 m). Different levels of loss of strands in the bottom flange (up to 25% loss) were simulated on both structures, and various repairs were applied in each case. Similarly, different levels of top flange damage were introduced in both structures up to 50% loss of the top flange. CFRP repairs applied on the soffit and the webs were examined in conjunction with the partial splicing of the severed strands for bottom damage cases.

3.2 Verification Using Finite Element Modeling

A 3D finite element model using Abaqus/Explicit software was developed to investigate the stress distribution before and after damage in an example prestressed girder. A rectangular section with a depth of 36 in and a width of 10.25 in (roughly equivalent to an AASHTO Type II girder with respect to height, area, and moment of inertia) was selected. Prestressing area was equivalent to a 16-strand tendon (0.6-in diameter each). The centroid of prestressing steel was located 6.75 in (171.5 mm) above the beam soffit (Figure 8). Span length was selected to be 50 ft (15.24 m).

Three-dimensional deformable solid elements were used to model the concrete and prestressing tendons (Figures 9 and 10). Taking advantage of symmetry (axis of symmetry in the z direction at mid-span), only half of the span length was modeled for the simulation. End support was defined by constraints in x and y directions. Both concrete and steel were modeled as linear elastic materials. Material properties are shown in Table 1.

The interaction between steel and concrete including normal, tangential and cohesive behavior was modelled to simulate the transfer of forces at the steel-concrete interface. To simulate the bond at the interface of steel and concrete, steel was treated as the master surface and the concrete as the slave surface. The concrete also had a finer mesh than that of the steel, as suggested by the Abaqus user manual.

Prestressing forces was specified as a predefined field stress in the longitudinal direction of the strands, considering the effective stresses in each strand, and accounting for the calculated effects of long-term relaxation, shrinkage, and creep. Elastic shortening was modelled through the finite element model itself. The model change technique was used to simulate a damage scenario in the beam. The damage was introduced at (and near) midspan as shown in Figure 11.

Prestressing was represented as a predefined field stress at the initial state in the strands. The analysis was performed in two steps following the initial state. Step 1 included application of girder self-weight as gravity

load and transfer of prestressing force from steel to the concrete. Step 2 involved initiation of damage (removal of elements) in the model.

Figure 11 shows the longitudinal stress contour in the beam at the end of step 2. The stresses before and after damage (stress change due to damage) at four corners points of the section at midspan were calculated and compared with the calculations using the equations proposed in this chapter.

The transformed section properties calculated for the undamaged and damaged sections are shown in Table 2, without considering the secondary effects due to upward camber of the beam. The secondary $P-\Delta$ effect due to camber can be handled in the calculations by increasing the Δe_y value by the amount of vertical deflection as the beam undergoes change from undamaged to damaged condition. Moments due to dead load and effective prestressing force for the considered section are calculated as shown in Table 3.

Using above properties and forces (Tables 2 and 3), and Equation 13, stress change due to damage in the section can be calculated. Table 4 shows the stress changes using (Equation 13) and results from the Abaqus model at points A, B, C, and D with or without consideration of secondary effects. The results show reasonable agreement between calculated and finite element results. The remaining differences are mainly due to other secondary effects that are not considered in the calculations. These secondary effects are normally not considered in the design process for prestressed bridge members.

3.3 Example

Table 5 shows calculated stresses before and after introduction of damage on a 72-in (1.828 m) deep Wisconsin Type 72W section with a span length of 146 ft (44.5 m). The girder spacing was 7.5 ft (2.286 m), and a structural slab thickness of 7.5 in (191 mm) was used (with a total slab thickness of 8 in or 203 mm including wearing surface). Forty-six 0.5-in. (12.7-mm) Grade 270 low relaxation strands were used in the bottom flange. The design compressive strengths for girder and slab concrete were 6.8 ksi (46.9 MPa) and 4.0 ksi (27.6 MPa), respectively. The strands were draped based on Wisconsin practices. The damage

was assumed to occur at mid-span. Additional details for this example are provided by Tabatabai and Nabizadeh (2019).

Calculations were performed using the PreBARS software. The damage introduced included loss of 11 strands (24%) as shown in Figure 7. Results in Table 5 indicate that the introduction of damage increased compressive stresses in the deck slab and the top of the girder, and substantially higher tensile stresses were generated in the bottom flange. The stress at the bottom of the beam was 205 psi (compression) under permanent and transient loads prior to damage. This bottom stress reversed sign and increased to 753 psi (tension) following the damage. The maximum compressive stress at the top of the girder increased from 3.03 ksi to 3.33 ksi because of the damage.

4.0 SUMMARY AND CONCLUSIONS

To properly assess the structural condition of accidentally damaged prestressed bridge girders, it is important that the girder's condition be carefully assessed in the field and calculations be performed for both serviceability and strength limit states. Prior research efforts have focused on strength calculations and have not addressed procedures for serviceability stress checks following accidental damage to prestressed bridge girders. The following is a summary of the work and its findings:

- A methodology has been developed to calculate stress changes in damaged prestressed bridge girders using a differential approach that considers the redistribution of stresses in a generalized unsymmetrical composite section. These procedures apply equally to cases of bottom or top flange damage in prestressed girders.
- An approach involving the use of spreadsheets (PreBARS software) was adopted to calculate undamaged and damaged section properties and the resulting stress changes using the developed procedures. In a graphical representation of the cross section, each cell in the spreadsheet represented a 0.5-in x 0.5-in (12.7 mm x 12.7 mm) square. To introduce damage, the user would

“zero-out” the cells that have been damaged/spalled/severed. The undamaged and damaged section properties and the stress calculations are then performed by the spreadsheet.

- Verification of the developed theoretical procedures was provided through a 3-dimensional nonlinear finite element model of a prestressed concrete beam. A comparison of stress results at selected points showed reasonably good agreement, especially when the secondary effects of eccentricity (due to beam camber) were considered.
- The development of these theoretical methods and software tools allows bridge engineers to perform the required serviceability stress checks in damaged prestressed bridge girders. Further research is needed to assess the applicable stress limits under damaged conditions.

Acknowledgements

The project team appreciates the support of the Wisconsin Highway Research Program (WHRP) in sponsoring this research project. We especially thank Mr. William Oliva, Mr. David Kiekbusch, and Mr. Aaron Bonk of the Wisconsin Department of Transportation and other members of the project oversight committee for their help and input.

Funding Statement

This research was funded through the Wisconsin Highway Research Program by the Wisconsin Department of Transportation and the Federal Highway Administration under Project 0092-17-02. The contents of this paper reflect the views of the authors who are responsible for the facts and accuracy of the data presented herein. The contents do not necessarily reflect the official views of the Wisconsin Department of Transportation or the Federal Highway Administration at the time of publication.

Conflict of Interest

The authors have no conflict of interest to report. Habib Tabatabai is an Editorial Board Member of this journal but was not involved in the peer-review process nor had access to any information regarding its peer-review.

Author Contributions

Conception, H.T. and A.N.; Performance of work, A.N. and H.T.; Interpretation of data, H.T. and A.N.; writing the article, H.T. and A.N. Both authors have access to data.

REFERENCES

- [1] Shanafelt, GO, Horn, WB. Guidelines for Evaluation and Repair of Prestressed Concrete Bridge Members. National Cooperative Highway Research Program (NCHRP) Report 280, National Research Council, Washington, D.C. November 1985, 84 pp.
- [2] Tabatabai, H, Nabizadeh, A. Strength and Serviceability of Damaged Prestressed Girders. Report No. 0092-17-02, Wisconsin Highway Research Program, Wisconsin Department of Transportation, May 2019, pp 214.
- [3] Nabizadeh, A, Tabatabai, H. Assessment and Repair of Damaged Prestressed Girders. Proceedings of the Bridge Engineering Institute (BEI) conference, Honolulu, Hawaii, August 2019.
- [4] Shanafelt, GO, Horn, W.B. Damage Evaluation and Repair Methods for Prestressed Concrete Bridge Members. National Cooperative Highway Research Program (NCHRP) Report 226, National Research Council, Washington, D.C., November 1980, 66 pp.
- [5] Tadros, M, Baishya, MC. Rapid Replacement of Bridge Decks. National Cooperative Highway Research Program (NCHRP) Report 407, National Research Council, Washington, D.C., 1998, 52 pp.

- [6] Harries, KA. Full-scale Testing Program on De-Commissioned Girders from the Lake View Drive Bridge, Report to the Pennsylvania Department of Transportation. FHWA-PA-2006-008-EMG001 University of Pittsburgh, 2006, 147 pp.
- [7] Harries, KA, Kasan, JL, Aktan, C. Repair Method for Prestressed Girder Bridges. Report No. 2009-008-PIT 006, Pennsylvania Department of Transportation, June 2009.
- [8] Assad, S. Evaluating the Impact of Bridge Deck Removal Method on The Performance of Precast/Prestressed Concrete I-Girders. master's thesis, University of Nebraska, Lincoln, Nebraska, August 2014.
- [9] Kasan, JL. On the Repair of Impact-Damaged Prestressed Concrete Bridge Girders. PhD dissertation, University of Pittsburgh, 2012.
- [10] Feldman, LR, Jirsa, JO, Fowler, DW. Carrasquillo, RL. Current Practice in the Repair of Prestressed Bridge Girders. Report No. FHWA/TX-96/1370-1, Texas Department of Transportation, 1996, pp. 86.
- [11] Harries, KA, Kasan, J, Miller, R, Brinkman, R. Updated Research for Collision Damage and Repair of Prestressed Concrete Beams. Report prepared for the National Cooperative Highway Research Program, May 2012.
- [12] PCI. Bridge Design Manual. Publication No. MNL-133-11, 3rd edition, Precast/Prestressed Concrete Institute, Chicago, IL, 2011.
- [13] AASHTO. Standard specifications for highway bridges (LRFD). American Association of State Highway and Transportation Officials, Washington, DC; 2018.

Table 1. Material properties used in Abaqus model.

Material	Density lb/ft ³ (kg/m ³)	Modulus of elasticity ksi (MPa)	Poisson's ratio
Steel	485 (7,769)	28,500 (196,500)	0.3
Concrete	150 (2,403)	4,230 (29,165)	0.15

Table 2. Section properties for non-composite rectangular section before and after simulated damage

Parameter	Undamaged section	Damaged section	Δ
Area (in ²)	387.05	322.05	-65
I _x (in ⁴)	41888	30476	-11412
I _y (in ⁴)	3231	2477	-754
I _{xy} (in ⁴)	0	120	120
e _x (in)	0	0.29	0.29
e _y (in)	-10.47	-12.11	-1.64

Table 3. Moments and prestressing forces

P, kips (kN)	564 (2,509)	ΔP , kips (kN)	0
M_x , kip-in (kN-m)	1441.2 (162.8)	ΔM_x , k-in (kN-m)	0
M_y , kip-in (kN-m)	0	ΔM_y , kip-in (kN-m)	0
M_{Px} , kip-in (kN-m)	-6722.9 (-759.58)	ΔM_{Px} , kip-in (kN-m)	-1169.2 (132.10)
M_{Py} , kip-in (kN-m)	0	ΔM_{Py} , kip-in (kN-m)	163.56 (18.48)

Table 4. Comparison of stress change due to damage, with or without the secondary effect of deflection, with Abaqus results

Point	x in (mm)	y in (mm)	$\Delta\sigma$ ksi (MPa)	$\Delta\sigma$ ksi (MPa)	$\Delta\sigma$ ksi (MPa)
			Without secondary effect	Considering secondary effect	Abaqus
Point A	5.1 (129.5)	-13.5 (-342.9)	1.458 (10.053)	1.896 (13.07)	1.890 (13.031)
Point B	-5.1 (-129.5)	-13.5 (-342.9)	0.897 (6.185)	1.335 (9.205)	1.451 (10.004)
Point C	5.1 (129.5)	18.5 (469.9)	-0.209 (-1.441)	-0.418 (-2.882)	-0.524 (-3.613)
Point D	-5.1 (-129.5)	18.5 (469.9)	-0.770 (-5.309)	-0.978 (-6.743)	-0.970 (-6.688)

Table 5. Stress changes due to 24% prestressing strand loss in a 72-in (1.828 m) girder with 146 ft (44.5 m) span.

Condition	Under Permanent Loads		Under Permanent + Transient Loads	
	Max stress ksi (MPa)	Min Stress ksi (MPa)	Max stress ksi (MPa)	Min Stress ksi (MPa)
Top of Deck				
Undamaged	0.136 (0.94)	0.136 (0.94)	0.726 (5.01)	0.726 (5.01)
Damaged	0.452 (3.12)	0.580 (4.00)	1.031 (7.11)	0.580 (4.00)
Top of Girder				
Undamaged	2.388 (16.46)	2.388 (16.46)	3.031 (20.90)	3.031 (20.90)
Damaged	2.742 (18.91)	2.096 (14.45)	3.331 (22.97)	2.684 (18.51)
Bottom of Girder				
Undamaged	1.285 (8.86)	1.285 (8.86)	0.205 (1.41)	0.205 (1.41)
Damaged	0.728 (5.02)	0.000 (0.00)	0.000 (0.00)	-0.763 (-5.26)

Positive values denote compression.

Figure Captions

Figure 1. Modes of damage to prestressed girders: a) Accidental over-height vehicle impact; b) Unintended damage during deck slab removal

Figure 2. A concrete cross section with a prestressing force applied at its centroid

Figure 3. Transformed concrete cross section with the area of steel converted to concrete

Figure 4. Undamaged (a) and damaged (b) cross sections

Figure 5. Addition of area (A_g) with a subsequent loss in section due to damage (A_d)

Figure 6. Eccentric prestressing force applied on a cross section

Figure 7. Representation of undamaged and damaged girder section using PreBARS spreadsheet-based program

Figure 8. Cross-section of undamaged prestressed girder modelled in Abaqus

Figure 9. Cross sectional view of the undamaged rectangular prestressed beam

Figure 10. Three-dimensional view of the prestressed girder model

Figure 11. Damage simulation near the midspan of the beam (the cross section seen on the left is at midspan)

Figure 1. Stress contour after introduction of damage

Figure 13. Measurement points (A, B, C, D) for calculations of change in stress due to damage



(a)



(b)

Figure 1. Modes of damage to prestressed girders: a) Accidental over-height vehicle impact; b) Unintended damage during deck slab removal

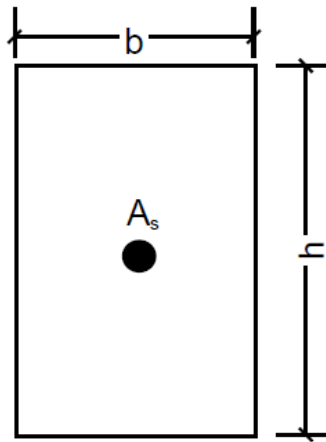


Figure 2. A concrete cross section with a prestressing force applied at its centroid

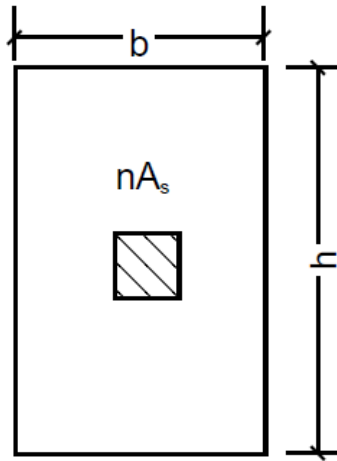
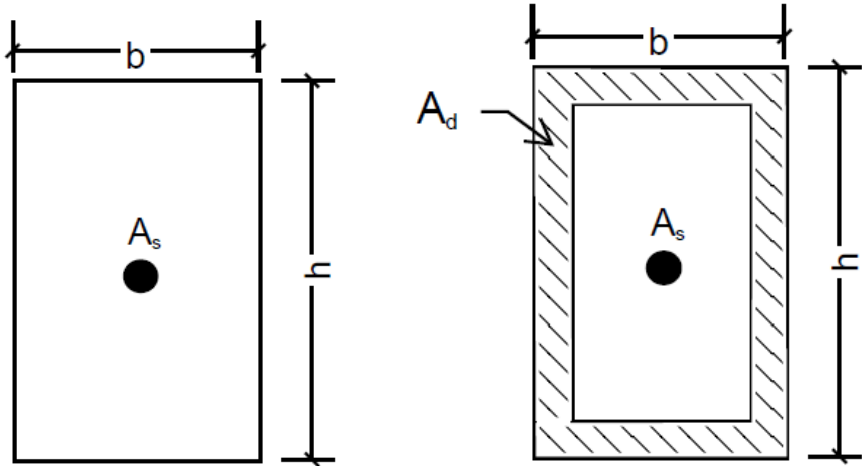


Figure 3. Transformed concrete cross section with the area of steel converted to concrete



a) Undamaged section

b) Damaged section (loss of A_d)

Figure 4. Undamaged (a) and damaged (b) cross sections

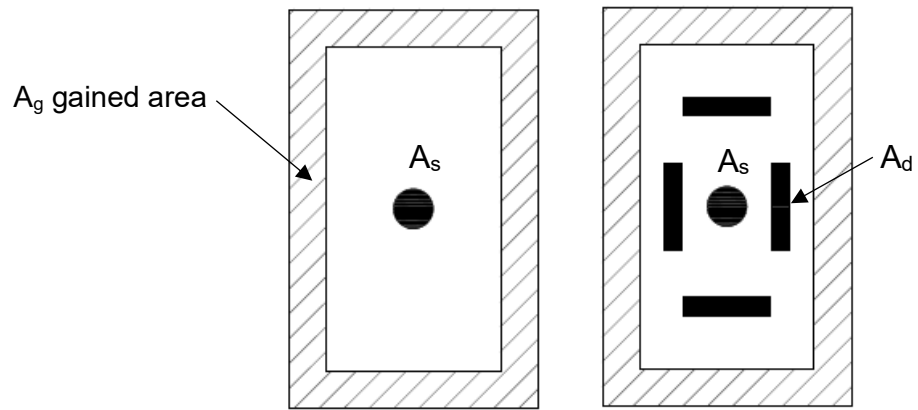


Figure 5. Addition of area (A_g) with a subsequent loss in section due to damage (A_d)

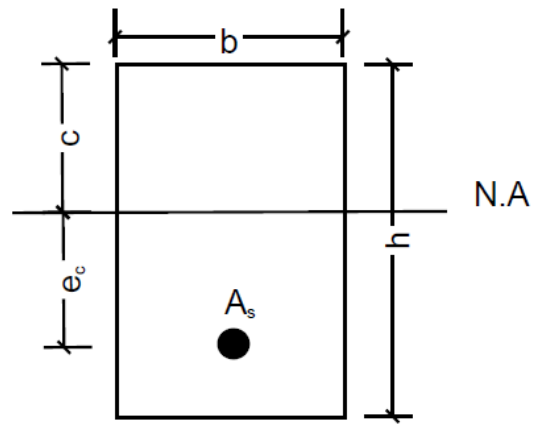
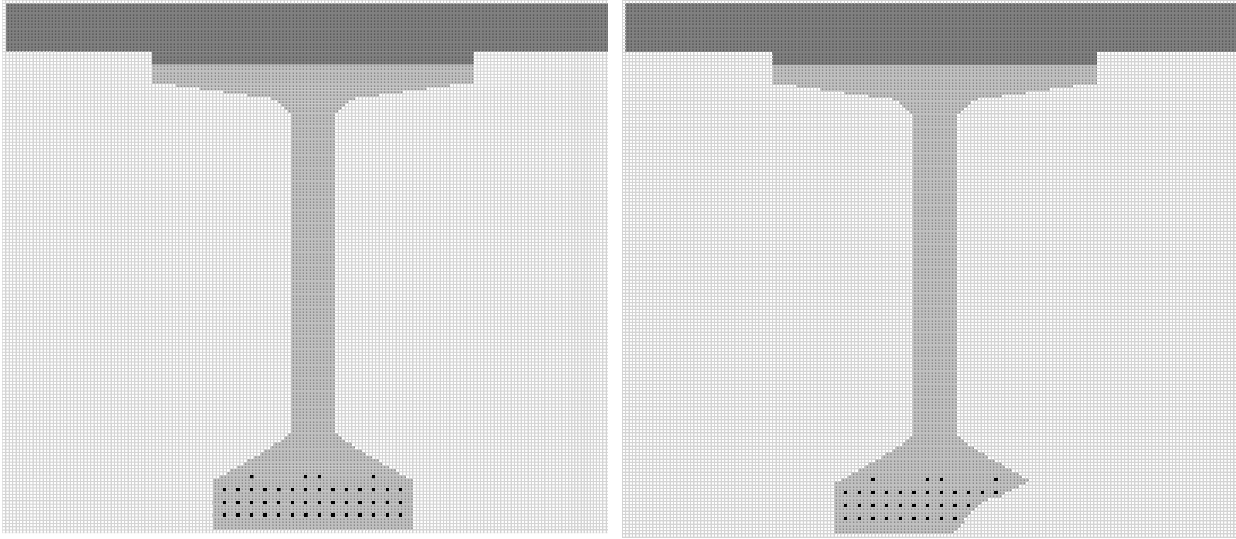


Figure 6. Eccentric prestressing force applied on a cross section



Undamaged Girder

Damaged Girder

Figure 7. Representation of undamaged and damaged girder section using PreBARS spreadsheet-based program.

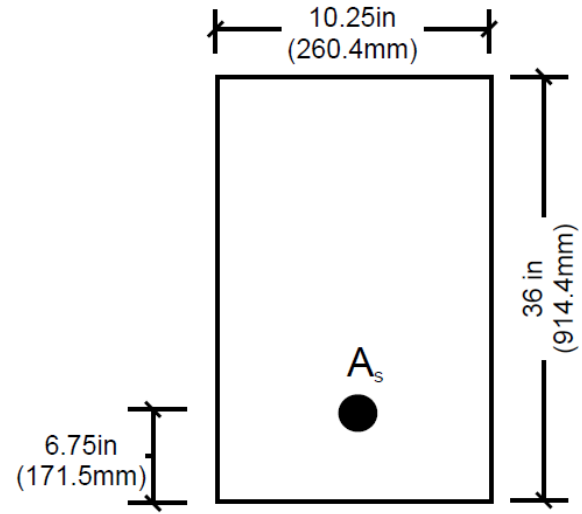


Figure 8. Cross-section of undamaged prestressed girder modelled in Abaqus

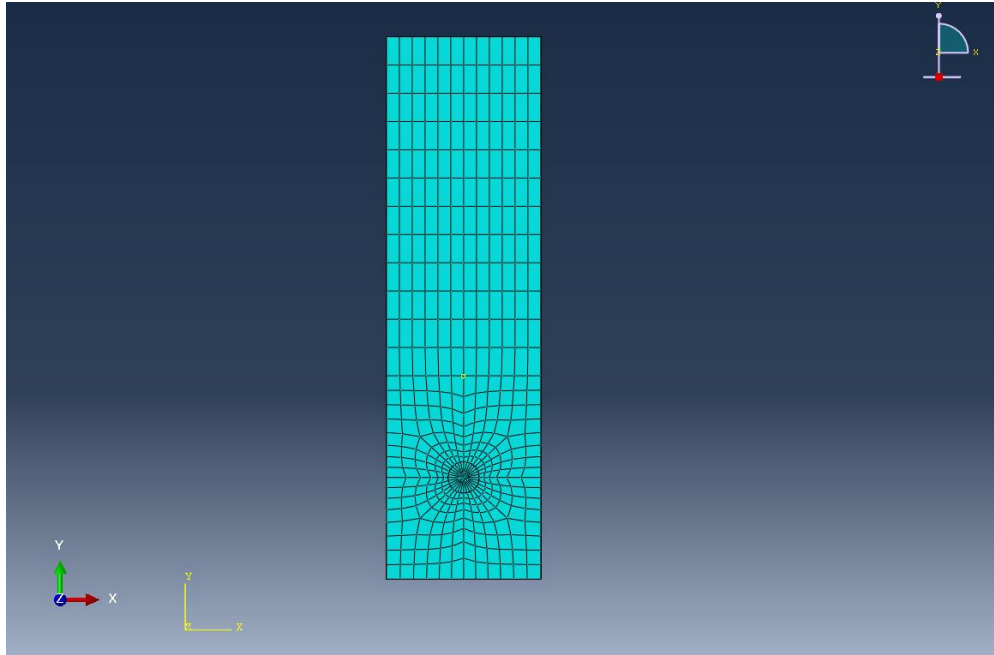


Figure 9. Cross sectional view of the undamaged rectangular prestressed beam

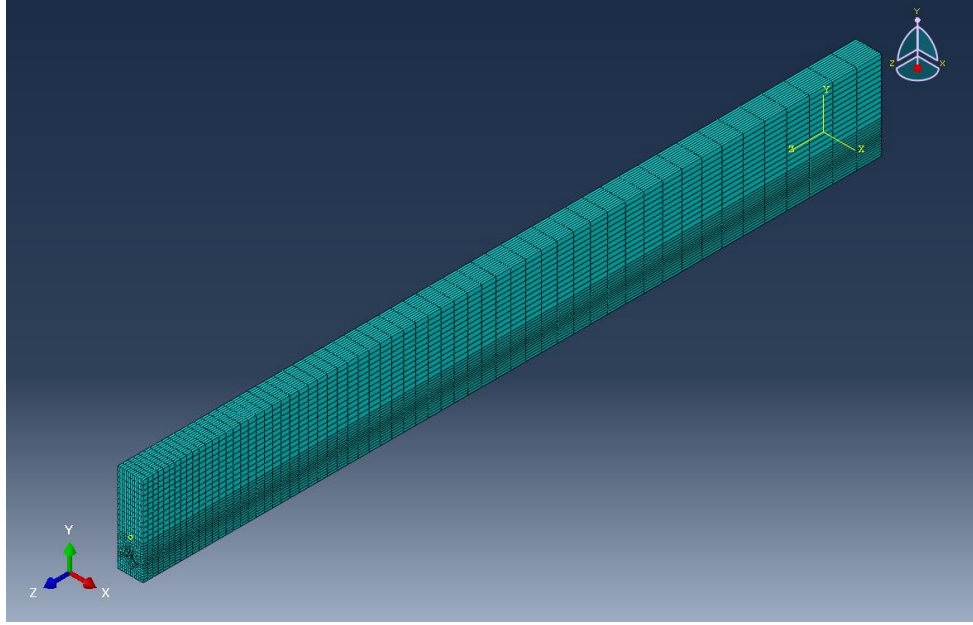


Figure 10. Three-dimensional view of the prestressed girder model

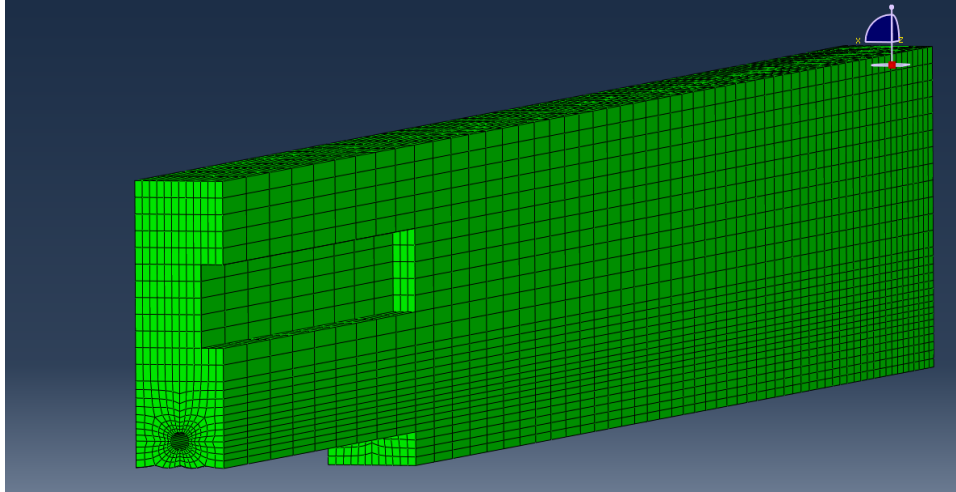


Figure 11. Damage simulation near the midspan of the beam (the cross section seen on the left is at midspan)

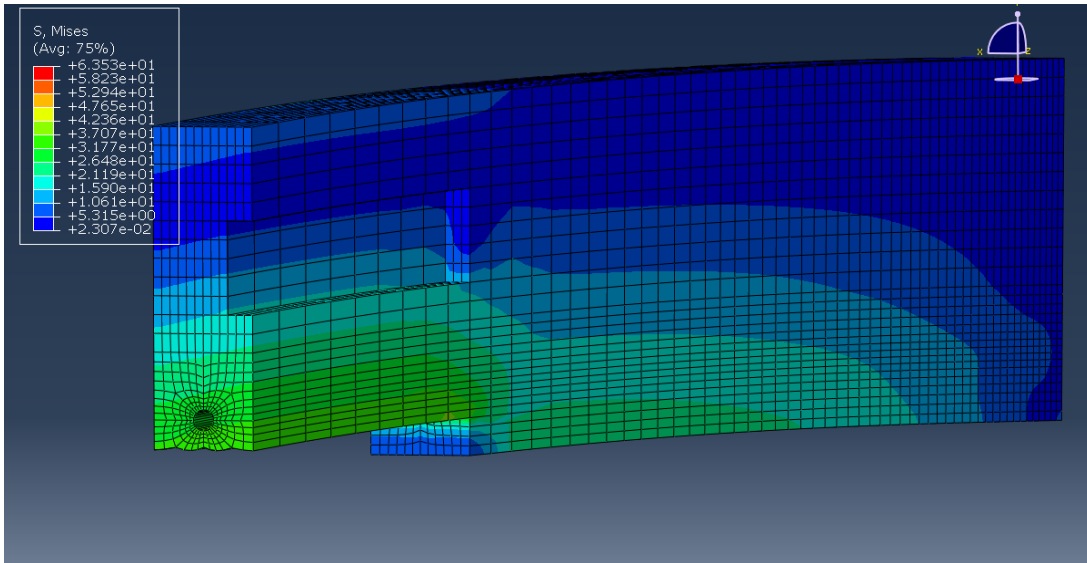


Figure 2. Stress contour after introduction of damage

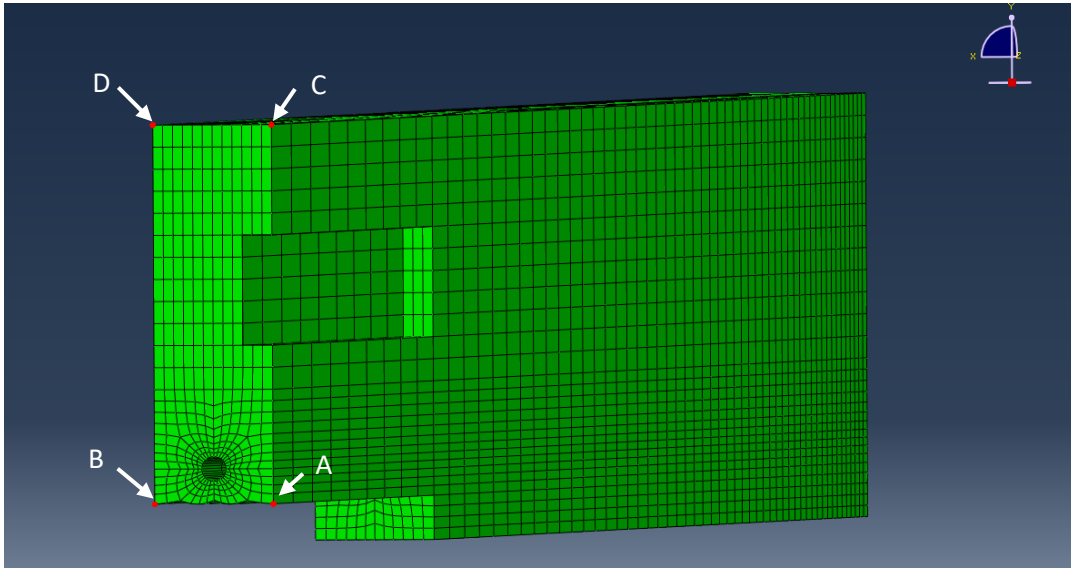


Figure 13. Measurement points (A, B, C, D) for calculations of change in stress due to damage